Krzysztof BERNACKI, Artur NOGA

Politechnika Śląska, Instytut Elektroniki

Influence of heat sink dimensions and source location on the radiated emission

Abstract. *In this paper, influence of heat sink dimensions and source location on radiated emission is presented. Some numerical and experimental results show radiated electric field for different heat sink configurations.*

Streszczenie. *W artykule omówiono wpływ zmiany lokalizacji pobudzenia i zmiany rozmiarów radiatorów na poziom emisji promieniowanej. Analizę przeprowadzono dla kilku konfiguracji źródła ciepła i radiatora, dla których pokazano wyniki pomiarów i obliczeń numerycznych.* ***(Wpływ rozmiarów radiatora i miejsca włączenia pobudzenia na poziom emisji promieniowanej)****.*

Keywords: Heat sinks, numerical modeling, electromagnetic compatibility, radiated emissions, EMI.
Słowa kluczowe: Radiatory, model numeryczny, kompatybilność elektromagnetyczna, zaburzenia promieniowane.

doi:10.12915/pe.2014.07.29

Introduction

The continuing growth of IC (Integrated Circuit) performance, i.e. scale of integration and clock speed, results in high power consumption. Nowadays, the power dissipated by the processors reaches level of 130W and still increases. It causes huge heat generation by modern IC (CPU, VLSI, ASIC, etc.). Each of them have a limited operating temperature, and usually the heat needs to be dissipated through a heat sink. On the other hand, the rapid switching capability of modern semiconductor devices results in very fast voltage and current variations. Therefore the high-speed IC may be the source of EMI (ElectroMagnetic Interferences). The capacitive couplings between IC and the heat sink are responsible for common-mode currents and voltages which act on conducting structures such as heat sinks [1]. Since, wavelength of these signals are comparable to heat sink dimensions, the heat sinks can be very effective non intuitive antennas. For this reason, heat sink design has become one of the major concerns in electromagnetic compatibility [1,2] of ICs and electronic modules.

The level of electromagnetic (EM) field radiated by heat sink depends on its mechanical and electrical properties. Since capacitive coupling is the main transfer path of signal noise, therefore the shape and dimensions of heat sink have influence on the EM field radiation [3,4]. It is worth noting, that apart from the width and length of heat sink, the distance between heat sink and ground plane is also very important [3]. On the other hand, the height of the heat sink has a very small influence on the emission level (up to 3 GHz) [5, 6]. The dimensions and the shape of heat sink fins are very important for heat dissipation, but usually have no influence on EMI [7, 8]. For this reason, the heat sinks usually can be effectively modeled by simple solid blocks [9, 10]. Since the dimensions of the heat sink and its distance to the ground plane are mainly determined by the dissipated power and IC package, radiated emission can be effectively reduced by appropriate grounding scheme, i.e. number and location of the grounding points [9,10].

The authors already presented the influence of the different heat sink configurations on radiated electromagnetic field [11-13]. It was shown that EMI does not depend significantly upon the fins structure (up to 3GHz) and the effect of heat sink fins can be ignored [11]. In [12] and [13] authors show that increasing number of ground points and its location near to the center of heat sink (i.e. noise source) cause reduction of radiated emission. It is worth noting, that decreasing of the distance between the heat sink and ground plane also enables to reduction of EMI [13].

In this paper, the influence of heat sink dimensions and source location on the radiated emission is presented. The particular attention is paid to the resonant frequencies of the heat sinks. The investigations are based on numerical simulations and measurements. Some numerical and experimental results for few heat sink configuration are also presented.

Methods

As was mentioned, the investigation is based on the simulations in time domain and measurements. For numerical purposes CST Microwave Studio program is used, where efficient full-wave FIT (Finite Integration Technique) is employed [14]. The heat sink with dimensions 84×78×50 mm (length×width×height) (basic configuration) is made of PEC (Perfect Electrical Conducting) object and located 12 mm above a square ground plane with side length 300 mm.

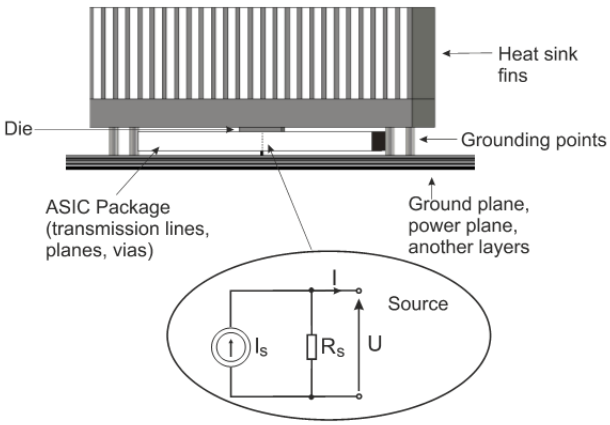

Fig.1. Simplified view of considered object and adopted equivalent circuit

Fig. 1 shows (e.g.) general simplified view of considered object and adopted equivalent circuit. The ground plane is modeled by single layer FR4 laminate (ε_r= 4.3, tanδ = 0.025). The source, that represents the interferences generated by VLSI device, is modeled by discrete port defined between the heat sink and ground plane. The discrete port is modeled by a lumped element, consisting of a current source with an inner impedance (R_s=50 Ω) and output power of 1 W (see Fig. 1). The testing configurations are analyzed from 30 MHz to 3 GHz. It is worth noting, that for this frequency band radiated electric field does not depend significantly upon the fins structure [3,11]. It means that heat sinks can be effectively modeled by simple solid

blocks. It is advantageous for numerical calculations, because it usually means reduction of computer resources required to perform computations.

The shapes and sizes of heat sinks used for measurements correspond to numerical models. For experiments, the heat sinks are made of the aluminum (EN AW-5083). The scheme of the test setup for measurement consists of device under test (DUT – heat sink with the ground plane), vector network analyzer (Agilent N5230A) and antenna (Ultralog HL562 Rohde\Schwarz) [12]. Distance between antenna and DUT (on the isolating support 0.8 m above the ground) is 3 m [15]. The heat sink is excited by one port of the vector network analyzer (VNA) in the range from 30 MHz to 3 GHz with - 8dBm output power. The receiving antenna is connected to second port of VNA. It is assumed, that all measurements are for horizontal polarization and fixed antenna height (1.2 m above ground) - for this polarization the largest level of electric field was detected. Experimental model is presented in the Fig. 2.

The radiated emission from the heat sink are measured by VNA in terms of dB. Therefore the antenna factor AF (dB) and cable loss CL (dB) are applied to the measurement data to obtain the radiated electric field amplitude in dBμV/m. Based on measurement data (S_{21}) the electric field *E* can be obtained as follow

$$E(dB\mu V/m) = S21(dB)+AF(dB)+CL(dB)+\mathrm{F(dB)} \quad (1)$$

where *F* is factor that allows conversion *dB to dBμV*. The example values of *F*, *AF* and *CL* are presented in Tab. 1. It should be noted, that because of differences between the output power (30 dBm for simulations and -8 dBm for measurements) numerical results are normalized. This allows one to direct comparison of numerical and experimental results.

Fig. 2. Experimental model of heat sink

Table 1. Antenna factor and cable loss for selected frequencies

F (GHz)	AF (dB)	CL (dB)
0.35	12.36	1.62
0.6	17.00	1.81
0.85	20.05	2.06
1.1	22.63	2.30
1.35	24.29	2.55
1.6	26.37	2.79
1.85	27.14	3.01
2.1	27.90	3.23
2.35	29.22	3.48
2.6	29.98	3.65
2.85	31.22	3.87
3.0	31.34	3.99

Numerical and experimental results

Firstly the influence of the source location on the radiated emission is presented. In this paper, two configurations are considered, i.e. source located at the center of the heat sink – 'Setting 1', and the source mounted near the corner of the heat sink – 'Setting 2' (see Fig. 3). Amplitude of the radiated electric field obtained by numerical simulations and measurement is presented in Fig. 4 and Fig. 5, respectively. We can see, that emission level is lower for system with the source located at the heat sink center. The difference between analyzed configurations reaches 13 dB in the worst case.

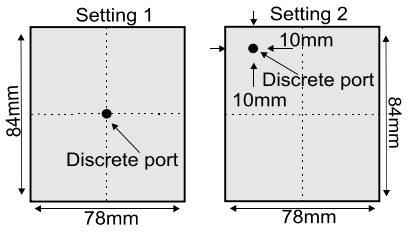

Fig. 3. Source location - analyzed settings

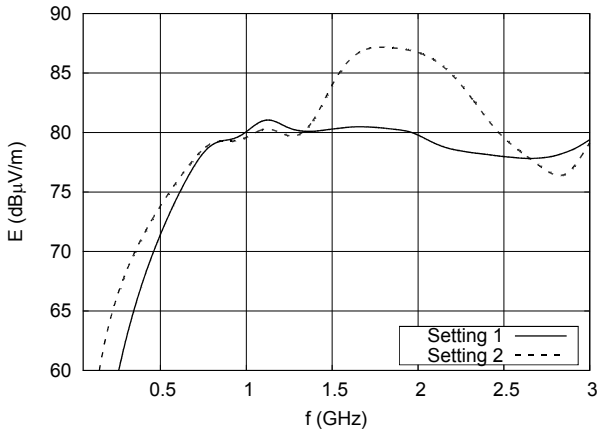

Fig. 4. Influence of the port location - numerical results

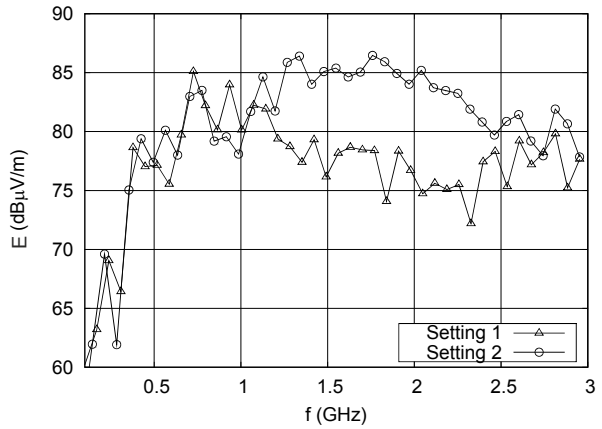

Fig. 5. Influence of the port location – measurements

It is obvious, that increased radiation level is observed at the resonant frequencies. Resonances due to the geometrical dimensions of the heat sink are expected at the following frequencies

$$(f_r)_{m,n,p} \approx \frac{c}{2\pi\sqrt{\varepsilon_r}}\sqrt{\left(\frac{m\pi}{X}\right)^2+\left(\frac{n\pi}{Y}\right)^2+\left(\frac{p\pi}{h}\right)^2},(Hz) \quad (2)$$

where *c* is the speed of light, *m*, *n*, *p* denotes the number of half-cycle field variations along *x*, *y*, *z* directions, respectively. *X* and *Y* represent dimensions of the heat sink (length x width) along *x* and *y* directions, whereas *h* is distance between heat sink and ground plane. Since *h* is very small ($h<<\lambda$, where λ is wavelength), the field along *z* direction can be usually considered constant, and the resonance frequencies (modes) are primarily determined by dimensions *X* and *Y*. It is worth noting, that a mode excitation depends on source position. In other words, for a

given source location only some modes are excited and increased emission level is observed only at these resonant frequencies. For configuration called Setting 2, high emission levels are observed from 1.5 GHz to 2 GHz. It is obvious, because when the excitation source is located near corner of the heat sink, the following modes are excited: f_{100}≈1.8 GHz, f_{010}≈1.9 GHz.

The next example demonstrates the influence of the heat sink dimensions on the radiated emission. Fig 6 and 7 shows amplitude of the electric field obtained by numerical methods and measurements, respectively. Now, two heat sinks are analyzed: basic configuration with dimensions 84×78×50 mm, and the second one, where the one side is doubled, i.e. 84×156×50 mm. The source is located at the center of heat sink. We can observed increased levels of radiation at 1.9 GHz for the larger heat sink. Difference between results at this frequency exceeds 10 dB (see Fig. 7). When the source is located at the center of the heat sink, the mode f_{020} is excited in the analyzed frequency range. For the heat sink with dimensions 84×156×50 mm, the resonant frequency for this mode is about 1.9 GHz.

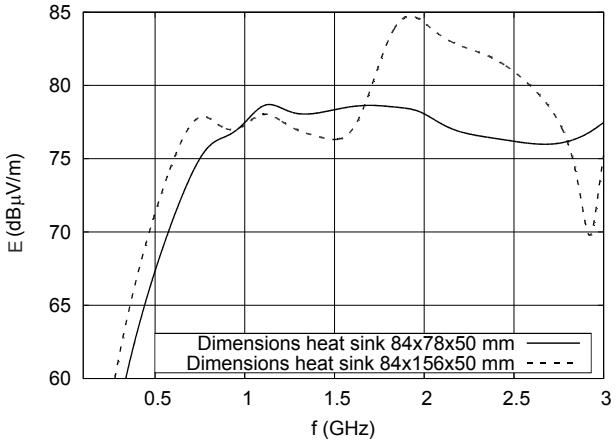

Fig.6. Influence of the heat sink dimensions - numerical results

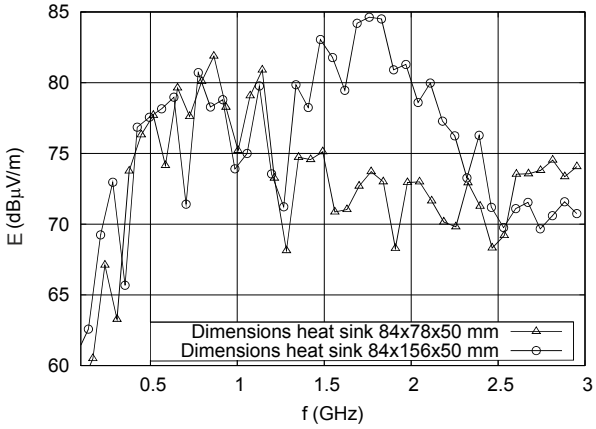

Fig. 7. Influence of the heat sink dimensions - measurements

Until now, all presented results are obtained at fixed observation point (r = 3 m, φ = 0°, θ = 90°). It means that not always the maximum value of radiated field is measured/calculated [11]. At low frequencies the observation point is at direction of maximum radiation (i.e. at θ=90°). Unfortunately, above 0.5 GHz the direction of maximum radiation varies from θ=90° to θ=20° and unintentional antenna (heat sink) is more directional [11]. For this reason, to accurate analysis of radiated emission at resonant frequencies, the additional numerical results are presented. The simulations is based on far field calculations. At each interesting frequency, the electric field is evaluated on a virtual sphere of 3 m and then the maximum of the electric field vector is saved. This procedure allows to determine the maximum value of the radiated emission in the analyzed frequency range.

The first structure analyzed in this way is the heat sink (84×78×50 mm) located 1 mm above a ground plane. The simulations are performed for source located alternatively at the point A, B and C (see Fig. 8). Now, range of analysis is extended up to 4.5 GHz. The resonant frequencies for the first seven modes are presented in Tab. 2. The columns 1 and 2 indicate the mode number. The theoretical resonant frequencies, listed in column 3 of Tab .1, are calculated by formula (2). The column 4 shows resonant frequencies obtained from numerical simulations, whereas columns 5, 6 and 7 list the value of real part of the input impedance for A, B and C source location, respectively. In the last three columns, *x* indicates that this mode is not excited. The maxim electric far field at a distance of 3 m versus frequency for different source position is presented in Fig. 9. Fig. 10 shows real part of input impedance calculated at the source terminals. The subscripts A, B and C in Figures labels indicate the appropriate source position. The Figures make it easy to check which modes are excited for each source position.

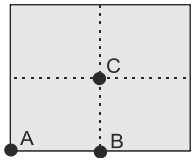

Fig.8. Source position - bottom side of heat sink

Table 2. Resonant frequencies in GHz (heat sink - 84×78×50 mm)

m	n	f_{rth}	$f_{r,num}$	R_A (Ω)	R_B (Ω)	R_C (Ω)
1	0	1,78	1,73	266	x	x
0	1	1,92	1,87	210	195	x
1	1	2,62	2,55	402	x	x
2	0	3,57	3,47	124	127	140
0	2	3,85	3,73	114	114	111
2	1	4,06	3,94	289	266	x
1	2	4,24	4,12	219	x	x

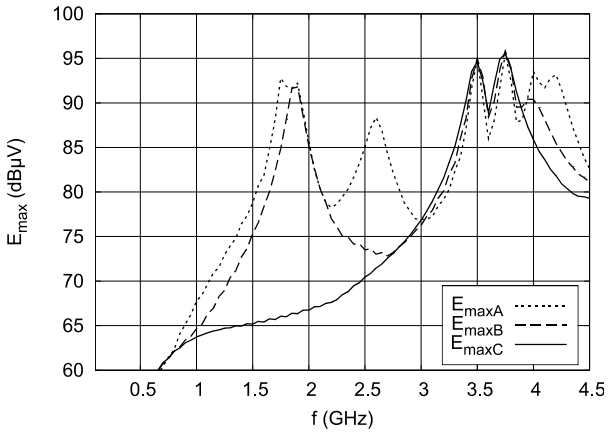

Fig. 9. Maximum radiated electric field at a distance of 3m for a different source location (heat sink 1 mm above ground plane)

The second analyzed structure is the heat sink with the same size but located 12 mm over a ground plane. The maximum radiated field at the distance of 3 m and real part of input impedance are presented in the Fig. 11 and 12, respectively. Comparing the results, one can see that for heat sink placed 1 mm above the ground plane, the resonant frequencies determined numerically are in very good agreement with theoretical data (see the columns three and four in Tab. 2). This is a highly resonant structure

exhibiting sharp peaks in their frequency response. This means that formula (2) can be used to accurately determine the resonant frequencies, where the maximum of radiated emission is observed. For this configuration, a significant reduction of radiation is observed out of resonance. As one can see, the best source location is position C - the heat sink placed central over the IC - when the smallest number of modes are excited. On the other hand, increasing the distance between heat sink and ground plane causes reduction of structure quality factor (see Fig. 12). The resonant frequencies obtained numerically do not correspond exactly with these obtained by (2). Additionally, we can observe increasing emission level in the all analyzed frequency range. It is due to the small differences between level of radiation at resonant frequencies and at other frequencies.

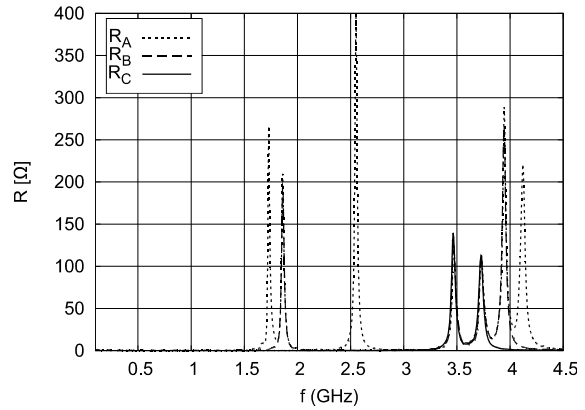

Fig. 10. Real part of input impedance at source terminals for different source positions (heat sink 1 mm above ground plane)

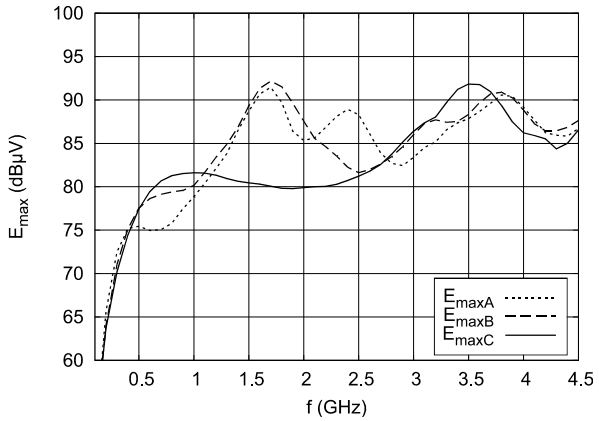

Fig. 11. Maximum radiated electric field at a distance of 3m for a different source location (heat sink 12 mm above ground plane)

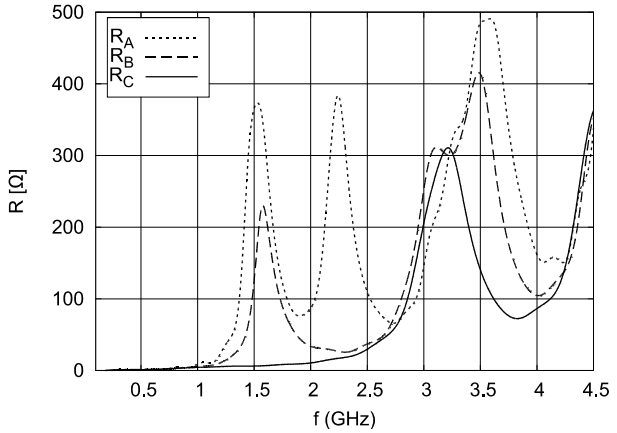

Fig. 12. Real part of input impedance at source terminals for different source positions (heat sink 12 mm above ground plane)

Conclusion

This paper shows the results of numerical and experimental analysis of electric field radiated by the objects with heat sink. This problem is presented for few testing configurations involving a change of excitation and dimensions of the heat sink. The results show, that the correct heat sink installation, i.e. in the center of the IC package, enables to reduce the level of radiation. The attention should also be paid to the size of heat sink. If the signal (clock) spectrum contains the heat sink resonant frequencies it can results in increased radiation level.

LITERATURE

[1] Joffe E., Kai-Sang L., Grounds for grounding, Wiley-IEEE Press, 2010.

[2] Bogatin E., Signal and Power Integrity – Simplified, Prentice Hall, 2010.

[3] Brench C. E., Heatsink radiation as a function of geometry, *IEEE International Symposium on Electromagnetic Compatibility* Aug. 1994, pp.105-109.

[4] Das S. K., Roy T, An investigation on radiated emissions from heatsinks, *IEEE International Symposium on Electromagnetic Compatibility*, vol.2, str. 784- 789, 1998, Denver, USA.

[5] Georgeria R., Montrose M., Product Safety and the Heat Sink - Dilemma of Minimizing Radiated Emissions and Maximizing Thermal Cooling, Electromagnetic Compatibility, 2003 IEEE International Symposium on, vol.1, pp.134-137, 18-22 Aug. 2003.

[6] Sochpux P., Yu J., Bhobe A., Centola F., Heat Sink Design Flow for EMC, *DesignCon 2008*, Feb. 2008, Santa Clara, USA.

[7] Lu J., Dawson F., EMC computer modelling techniques for CPU heat sink simulation, *3rd International Conference on Computational Electromagnetics and Its Applications*,1-4 Nov. 2004, pp. 272- 275.

[8] Manivannan S., Arumugam R., Devi S. P., Paramasivam S., Salil P., Subbarao B.: Optimization of heat sink EMI using Design of Experiments with numerical computational investigation and experimental validation, *IEEE International Symposium on Electromagnetic Compatibility*, 25-30 July 2010, pp.295-300.

[9] Archambeault B., Pratapneni S., Zhang L., Wittwer., Comparison of various numerical modeling tools against a standard problem concerning heat sink emissions, Electromagnetic Compatibility, 2001. EMC. 2001 IEEE International Symposium on , vol.2, pp.1341-1346.

[10] Archambeault B., Pratapneni S., Wittwer D., A Proposed Set of Specific Standard EMC Problems To Help Engineers Evaluate EMC Modeling Tools.

[11] Bernacki K., Noga A., Numerical and Experimental Analysis of Radiated Emissions from Different Heat Sink Configurations, 22nd International Conference Radioelektronika 2013, 17-18 April, 2012, Brno, Czech Republic, pp. 45-47.

[12] Bernacki K., Noga A., Analiza wpływu połączeń radiatora z płaszczyzną odniesienia na poziomy emisji promieniowanej, *Przegląd Elektrotechniczny*, R. 89 NR 4/2013, pp. 36-39.

[13] Bernacki K., Noga A., Woźnica T., Analiza poziomu pól elektromagnetycznych promieniowanych przez układy z radiatorami, *Przegląd Telekomunikacyjny i Wiadomości Telekomunikacyjne*, nr 4/2012, str. 273-275.

[14] http://www.cst.com.

[15] PN-EN 55022, "Urządzenia informatyczne – Charakterystyki zaburzeń radioelektrycznych – Poziomy dopuszczalne i metody pomiaru".

***Authors**: mgr inż. Krzysztof Bernacki, Politechnika Śląska, Instytut Elektroniki, ul. Akademicka 16, 44-100 Gliwice, E-mail: krzysztof.bernacki@polsl.pl*

dr inż. Artur Noga, Politechnika Śląska, Instytut Elektroniki, ul. Akademicka 16, 44-100 Gliwice, E-mail: artur.noga@polsl.pl